

A Simple Scheme for Jitter Reduction in Phase-Differential Carrier Frequency Recovery Loop

Hyungsoo Lim and Dong Seung Kwon

A very simple and efficient scheme for jitter reduction is proposed for a carrier frequency recovery loop using phase differential frequency estimation, which estimates the current frequency offset based on the difference of the average phases of two successive intervals. Analytical and numerical results presented in this paper show that by simply overlapping the observation intervals by half for frequency offset estimations, both the steady-state and transient performances can be improved. The proposed scheme does not require any additional hardware circuitry, but results in improved performance even with reduced complexity.

Keywords: Jitter reduction, carrier frequency recovery.

I. Introduction

In closed-loop synchronization algorithms, an instantaneous synchronization error should be estimated for proper updates of local timing, phase, or frequency. Most synchronization loop design procedures usually focus on the designs of synchronization error detection algorithms and feedback loop filters [1]-[3]. In this paper, we propose a simple but efficient modification of the observation window control scheme that significantly improves the synchronization performance.

We consider a carrier frequency recovery loop for direct-sequence spread-spectrum (DS-SS) signals under additive white Gaussian noise. We assume a simple carrier frequency offset estimation algorithm is employed that estimates the current frequency offset based on the average carrier phases of two successive observation subintervals [4]-[8]. In most of the previous literature, a new observation window for carrier frequency offset estimation starts after the local oscillator frequency is updated according to the previous offset estimate. The observation intervals are not overlapped, so that the estimate is a random process whose mean is a function of the local frequency offset only over the observation interval. This scheme simplifies the analysis since the frequency offset estimator can be modeled as a simple function of the local frequency offset and an additive estimation error. In this paper, a simple modification is made such that the observation intervals for successive frequency offset estimations are overlapped by half. Analytical and numerical results show that the proposed modification improves in terms of both the steady-state frequency jitter variance and the convergence speed.

This paper is organized as follows. The conventional and proposed carrier frequency recovery schemes are described in detail in section II. In section III, analytical expressions for both

Manuscript received Dec. 08, 2004; revised Feb. 16, 2006.

Hyungsoo Lim (phone: + 82 42 860 1608, email: lim@etri.re.kr) was with Mobile Telecommunication Research Division and is currently with Digital Broadcasting Research Division, ETRI, Daejeon, Korea.

Dong Seung Kwon (email: dskwon@etri.re.kr) is with Mobile Telecommunication Research Division, ETRI, Daejeon, Korea.

the steady-state and transient performances of the two schemes are derived, while analytical and numerical results are presented and discussed in section IV. Finally, conclusions are drawn in section V.

II. Description of the Conventional Scheme and the Proposed Modification

Figure 1 shows a typical carrier frequency recovery loop structure for DS-SS signals. The input signal to the synchronization circuit is a complex baseband signal, usually oversampled for a digital matched filter. The pseudorandom noise (PN) code timing of the received signal is then coarsely acquired after the chip rate decimation, resulting in a chip timing offset within a fraction of the chip duration. After the coarse timing acquisition, the chip-rate samples are multiplied with a locally generated complex tone whose frequency is controlled according to the low-pass filtered carrier frequency offset estimates. The multiplier output signal is fed to both the fine PN code timing tracking loop and the carrier frequency recovery loop for further iterative refinement.

We assume that the simple phase-differential algorithm is employed for the residual carrier frequency offset estimation as in [4]-[8], which estimates the offset from the difference between the average phases of two successive correlations with the local PN code. In this paper, let us focus on the carrier frequency recovery and assume that the PN code timing is properly recovered so that the timing offset is negligible.

The operation of the conventional loop is illustrated in Fig. 2(a). Each interval observed for carrier frequency offset estimation consists of two subintervals, and the frequency offset Δf_k is estimated from the difference of the average phases $\bar{\theta}_k'$ and $\bar{\theta}_k''$ over the subintervals of the k -th observation interval. The offset estimation $\Delta \tilde{f}_{k,A}$ is then low-pass filtered to be used to update the local numerically controlled oscillator frequency [9]. In Fig. 2(a), $F(z)$ is the discrete-time Fourier

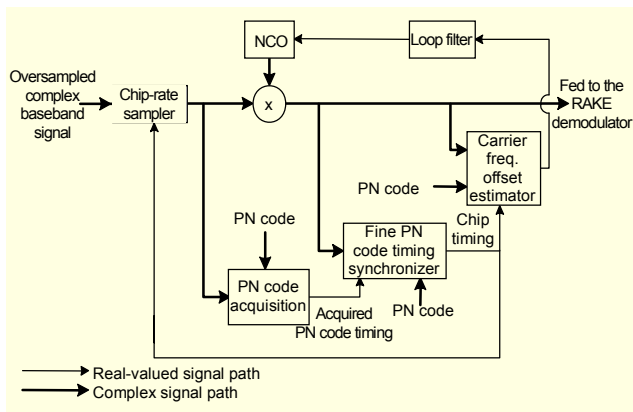


Fig. 1. Carrier frequency recovery loop structure under consideration.

transform of the impulse response of the loop filter, while f_k and $F(z)[g_k]$ denote the Heaviside operator as in [2], which is defined as

$$F(z)[g_k] = \sum_{m=-\infty}^{\infty} f_m g_{k-m} \quad (1)$$

for any discrete-time random process g_k .

In the conventional synchronization loop, the local carrier frequency is updated every two correlation intervals so that proper estimation can be made after the local carrier frequency update.

In order to mitigate the degradation due to the slow loop updates or the large delay in the loop [10], we propose to overlap the observation interval for successive estimations by half so that the local carrier frequency is updated every correlation interval, as shown in Fig. 2(b). The k -th and $(k+1)$ th carrier frequency offset estimates $\Delta \tilde{f}_{k,B}$ and $\Delta \tilde{f}_{k+1,B}$ are correlated since the input samples in the k -th correlation interval are used

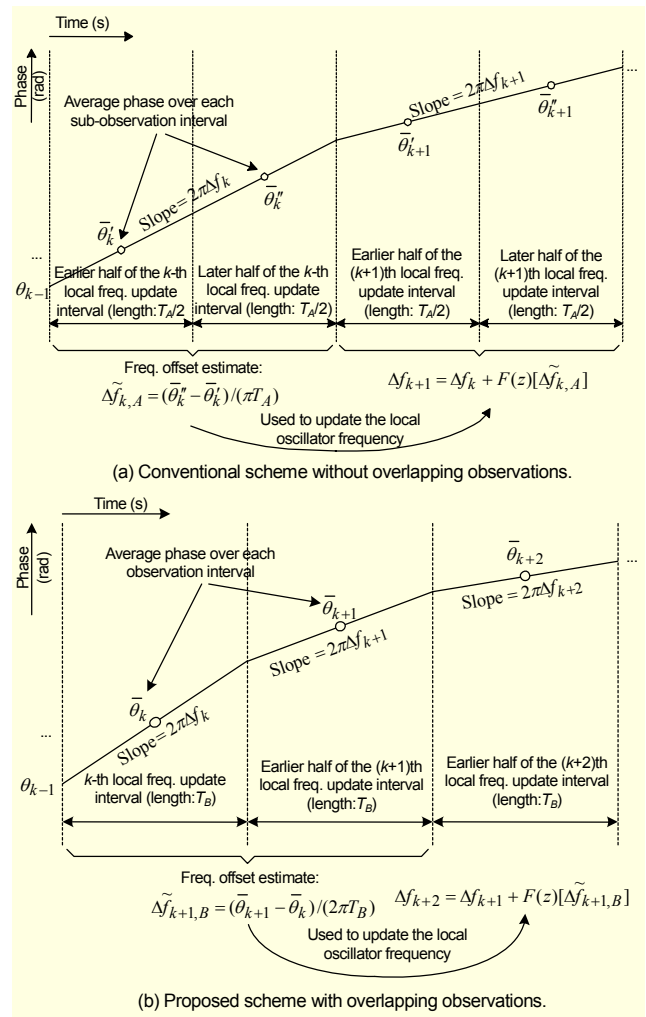


Fig. 2. Comparison of carrier frequency recovery loop operations.

in the calculation of both of them. The carrier frequency offset estimate in the loop is thus not a true estimate of an instantaneous offset but is rather a low-pass filtered version of it. It can be expected that the low-pass characteristics may improve both the steady-state jitter variance and loop convergence. The fast local frequency updates are also expected to improve the loop convergence further.

III. Steady-State and Transient Performance Analyses

In this section, we analyze the performance of the two carrier frequency recovery schemes for a unit-step input frequency offset under additive white Gaussian noise. As for the conventional scheme, both the first-order and second-order loops are analyzed since the proposed modification increases the loop order by one, as will be shown in section III.2.

1. Conventional Scheme

Let us first analyze the performance of the conventional scheme. The average carrier phases over the earlier and later halves of the k -th observation interval, $\bar{\theta}'_k$ and $\bar{\theta}''_k$, can be written as

$$\bar{\theta}'_k = \theta_{k-1} + \frac{\pi \Delta f_k T_A}{2} + n'_k \quad \text{and} \quad \bar{\theta}''_k = \theta_{k-1} + \frac{3\pi \Delta f_k T_A}{2} + n''_k, \quad (2)$$

respectively, where the observation interval length, T_A , is equal to the local carrier frequency update interval, θ_{k-1} and Δf_k are the initial carrier phase and local carrier frequency offset of the k -th observation interval, and n'_k and n''_k are the phase estimation errors for the earlier and later halves of the k -th interval, respectively. Under proper loop operation, the phase detector characteristic can be linearly approximated since the carrier frequency offset is small. The frequency offset estimate for the conventional scheme, $\Delta \tilde{f}_{k,A}$ obtained from the k -th observation interval, can then be written as

$$\Delta \tilde{f}_{k,A} = \frac{\bar{\theta}''_k - \bar{\theta}'_k}{\pi T_A} = \Delta f_k + \frac{n''_k - n'_k}{\pi T_A}, \quad (3)$$

and the phase estimation errors n'_k and n''_k can be approximated to be Gaussian with an identical variance equal to half of the reciprocal of the signal-to-noise ratio at the correlator output.

In case of the first-order loop, the local carrier frequency is controlled according to the frequency offset estimate as follows:

$$\Delta f_{k+1} = \Delta f_k - K_A \Delta \tilde{f}_{k,A}, \quad (4)$$

where K_A is the loop filter coefficient.

From (3) and (4), the transfer function of the loop can be obtained as

$$H_{A1}(z) = \frac{K_A}{z-1+K_A}, \quad (5)$$

and the unit-step response as

$$h_{A1}[k] * u[k] = [1 - (1 - K_A)^k] \cdot u[k], \quad (6)$$

where $h_{A1}[k]$ is the impulse response of the conventional first-order loop and $u[n]$ is the unit-step function. If we define the pull-in time as the time spent for the frequency offset to reduce to within $\pm 5\%$ of its initial value, the average pull-in time of the conventional first-order loop can be simply written as $T_A \log_{1-K_A} 0.05$ seconds.

From (5), we can also see that the loop is always stable and the mean squared carrier frequency offset converges to a unique value as $k \rightarrow \infty$ for all values of K_A within the practical range, $0 < K_A < 2$. Since the steady-state mean of the residual carrier frequency offset is zero, we can write the steady-state variance $\sigma_{\Delta f, A1}^2 = \lim_{k \rightarrow \infty} E\{\Delta f_{k+1}^2\}$ as

$$\begin{aligned} \sigma_{\Delta f, A1}^2 &= \lim_{k \rightarrow \infty} E\left\{\left[(1 - K_A)\Delta f_k - K_A \frac{\tilde{n}_k}{\pi T_A}\right]^2\right\} \\ &= (1 - K_A)^2 \sigma_{\Delta f, A1}^2 + \frac{K_A^2}{(\pi T_A)^2} \sigma_{\tilde{n}}^2, \end{aligned} \quad (7)$$

and thus

$$\sigma_{\Delta f, A1}^2 = \frac{K_A}{2 - K_A} \frac{\sigma_{\tilde{n}}^2}{(\pi T_A)^2}, \quad (8)$$

where $\tilde{n}_k = n''_k - n'_k$ and $\sigma_{\tilde{n}}^2 = E\{\tilde{n}_k^2\} = 2E\{n_k'^2\} = 2E\{n_k''^2\}$. As the variance of the estimation error is $\sigma_{\tilde{n}}^2 / (\pi T_A)^2$, the equivalent noise bandwidth of the loop [2] is

$$B_{A1} = \frac{K_A}{2 - K_A} \frac{1}{T_A}. \quad (9)$$

In the steady-state, the frequency offset is small enough such that $\sigma_{\tilde{n}}^2$ can be approximated as $\sigma_{\tilde{n}}^2 \approx 1/\gamma_c$, where γ_c denotes the signal-to-noise ratio at the correlator output.

Let us now consider a second-order loop where the difference equation and the loop transfer function are given by

$$\begin{aligned} \Delta f_{k+2} &= (2 - K_{A,P})\Delta f_{k+1} - (1 - K_{A,P} + K_{A,I})\Delta f_k \\ &\quad - \frac{1}{\pi T_A} [K_{A,P}\tilde{n}_{n+1} - (K_{A,P} - K_{A,I})\tilde{n}_k] \end{aligned} \quad (10)$$

and

$$H_{A2}(z) = \frac{K_{A,P}z - K_{A,P} + K_{A,I}}{z^2 - (2 - K_{A,P})z + 1 - K_{A,P} + K_{A,I}}, \quad (11)$$

respectively. If the equivalent noise bandwidth is sufficiently smaller than the loop update frequency $1/T_A$, the damping factor of the loop can be approximated as in [10] as

$$\zeta_A = \frac{K_{A,P} - K_{A,I}}{2\sqrt{K_{A,I}}}. \quad (12)$$

The unit-step response of the loop can be easily derived to be

$$h_{A2}[k] * u[k] = [1 - (1 - \beta_A)\alpha_{A+}^k - \beta_A\alpha_{A-}^k] \cdot u[k], \quad (13)$$

where $h_{A2}[k]$ is the impulse response of the conventional second-order loop and

$$\alpha_{A\pm} = \frac{2 - K_{A,P} \pm \sqrt{K_{A,P}^2 - 4K_{A,I}}}{2} \quad (14)$$

$$\text{and } \beta_A = \frac{1}{2} + \frac{K_{A,P}}{2\sqrt{K_{A,P}^2 - 4K_{A,I}}}. \quad (15)$$

Similarly to the previous manipulations, if the mean squared carrier frequency offset converges to a unique value as $k \rightarrow \infty$, we can write the steady-state frequency jitter variance as

$$\sigma_{\Delta f, A2}^2 = \frac{2(2 - K_{A,P})\sigma_{\text{cov}} + [K_{A,P}^2 + (K_{A,P} - K_{A,I})^2] \frac{\sigma_{\bar{n}}^2}{(\pi T_A)^2}}{1 + (2 - K_{A,P})^2 - (1 - K_{A,P} + K_{A,I})^2} \quad (16)$$

from (10), where $\sigma_{\text{cov}} = \lim_{k \rightarrow \infty} E\{\Delta f_{k+1} \Delta f_k\}$. Since we can also obtain

$$\sigma_{\text{cov}} = \frac{(2 - K_{A,P})\sigma_{\Delta f, A2}^2 - K_{A,P}(K_{A,P} - K_{A,I}) \frac{\sigma_{\bar{n}}^2}{(\pi T_A)^2}}{2 - K_{A,P} + K_{A,I}} \quad (17)$$

from (10), we finally have

$$\sigma_{\Delta f, A2}^2 = \frac{-2K_{A,P}^2 + 3K_{A,P}K_{A,I} - (2 + K_{A,I})K_{A,I}}{2K_{A,P}^2 - (4 + 3K_{A,I})K_{A,P} + (4 + K_{A,I})K_{A,I}} \frac{\sigma_{\bar{n}}^2}{(\pi T_A)^2}, \quad (18)$$

and the equivalent noise bandwidth is

$$B_{A2} = \frac{-2K_{A,P}^2 + 3K_{A,P}K_{A,I} - (2 + K_{A,I})K_{A,I}}{2K_{A,P}^2 - (4 + 3K_{A,I})K_{A,P} + (4 + K_{A,I})K_{A,I}} \frac{1}{T_A}. \quad (19)$$

2. Proposed Scheme with Overlapped Observations

In the proposed scheme, the average carrier phases over the k -th and $(k+1)$ th correlation intervals, $\bar{\theta}_k$ and $\bar{\theta}_{k+1}$, can be written as

$$\begin{aligned} \bar{\theta}_k &= \theta_{k-1} + \pi \Delta f_k T_B + n_k, \\ \bar{\theta}_{k+1} &= \theta_{k-1} + \pi (\Delta f_{k+1} + 2\Delta f_k) T_B + n_{k+1}, \end{aligned} \quad (20)$$

where T_B is the local frequency update interval length, which is equal to the correlation interval length, and n_k is the phase detector output noise component of the k -th correlation interval. The carrier frequency offset estimate for the proposed scheme, $\tilde{\Delta f}_{k+1, B}$, obtained from the k -th and $(k+1)$ th correlation intervals, can be written as

$$\tilde{\Delta f}_{k+1, B} = \frac{\bar{\theta}_{k+1} - \bar{\theta}_k}{2\pi T_B} = \frac{\Delta f_{k+1} + \Delta f_k}{2} + \frac{n_{k+1} - n_k}{2\pi T_B}, \quad (21)$$

and the local carrier frequency offset update equation is given by

$$\Delta f_{k+2} = \Delta f_{k+1} - K_B \tilde{\Delta f}_{k+1, B}, \quad (22)$$

where K_B is the loop filter coefficient.

From (21) and (22), the transfer function of the proposed loop is obtained to be

$$H_B(z) = \frac{K_B(z+1)}{2z^2 - (2 - K_B)z + K_B}. \quad (23)$$

It should be noted that the overlapping of observation windows increases the loop order by 1.

If the equivalent noise bandwidth is sufficiently smaller than the loop update frequency $1/T_B$, the damping factor of the loop can be approximated as

$$\zeta_B = \frac{2 + K_B}{4\sqrt{K_B}}. \quad (24)$$

From (23), we can obtain the unit-step response as

$$h_B[k] * u[k] = [1 - \beta_B \alpha_{B+}^k - (1 - \beta_B) \alpha_{B-}^k] \cdot u[k], \quad (25)$$

where $h_B[k]$ is the impulse response of the proposed loop,

$$\alpha_{B\pm} = \frac{2 - K_B \pm \sqrt{4 - 12K_B + K_B^2}}{4}, \quad (26)$$

and

$$\beta_B = \frac{1}{2} + \frac{2 - K_B}{2\sqrt{4 - 12K_B + K_B^2}}. \quad (27)$$

According to (23), within the practical range $0 < K_B < 2$, the proposed loop is also stable, and the mean squared carrier frequency offset converges to a unique value as $k \rightarrow \infty$ for all values of K_B . From (21) and (22), we can derive the steady-state variance $\sigma_{\Delta f, B}^2$ as

$$\sigma_{\Delta f, B}^2 = \frac{2K_B^2}{2 - K_B} \frac{\sigma_n^2}{(2\pi T_B)^2}, \quad (28)$$

and the equivalent noise bandwidth as

$$B_B = \frac{K_B^2}{2 - K_B} \frac{1}{T_B}. \quad (29)$$

From (8), (9), (18), (19), (28), and (29), we can see that the steady-state jitter variance is not guaranteed to be identical only by assuming identical equivalent noise bandwidths. In the next section, we additionally assume that either the steady-state jitter variance or the pull-in time is identical for fair comparisons between different schemes.

IV. Numerical Results

In this section, we compare the steady-state and transient performances of the two schemes considered via computer simulations. We assume that the chip rate is 4 Mchips/second and the chip signal-to-noise ratio is 0 dB. Throughout this section, all the loops are assumed to have an identical equivalent noise bandwidth [2] of 200 Hz, and the initial carrier frequency offset is given by 6 kHz. The steady-state frequency jitter variances presented in this section are measured over more than 40,000 local frequency updates after convergence. As a reference, we set the sampling frequency of the conventional loop equal to the chip rate.

First, we set $T_A = 2T_B$ to have an identical pull-in range, which is defined as the range of frequency offset that can be successfully converged to zero in the absence of noise and interference [3]. The pull-in ranges of the conventional and proposed schemes are $(-1/T_A, 1/T_A)$ and $(-0.5/T_B, 0.5/T_B)$ in Hz, respectively, which should outrange the initial carrier frequency offset. Since we assume the initial carrier frequency offset of 6 kHz, we choose the correlation length to be 32 chips for the conventional loop. The correlation length of the proposed loop should be 16 chips for the identical steady-state jitter variance of $3.96 \times 10^4 \text{ Hz}^2$, which can be easily derived from (8), (9), (28), and (29). In order to meet these conditions, we assume that 2:1 decimation is applied at the input to the carrier frequency offset estimator.

The simulation and analytical results are shown in Figs. 3(a) and 3(b), respectively. We can first verify that the analytical

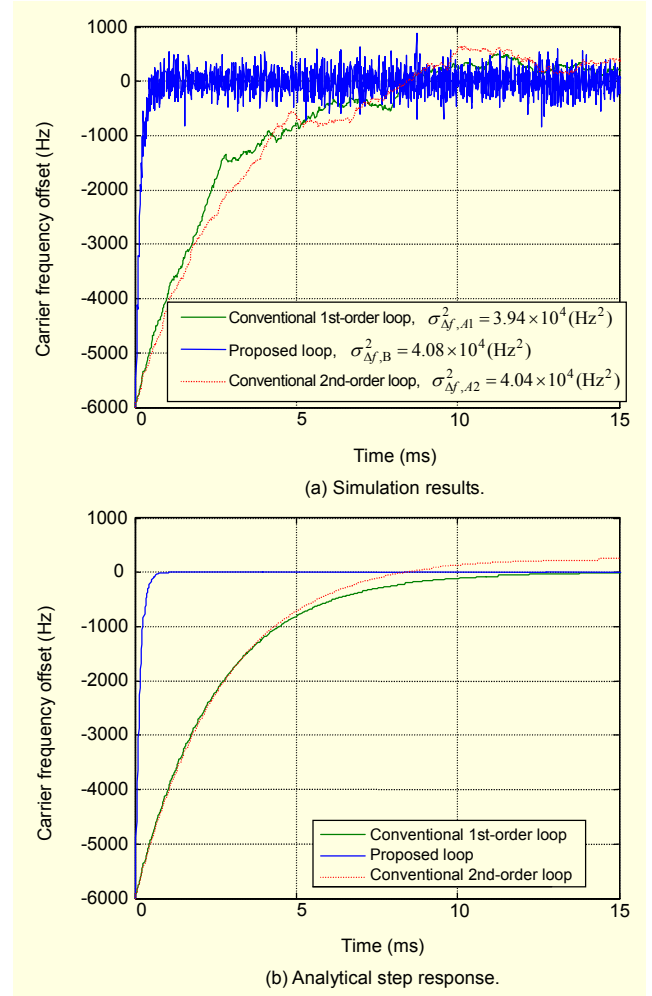


Fig. 3. Loop performances when the loops are designed for identical pull-in range of $(-6.25, 6.25)$ kHz, equivalent noise bandwidth of 200 Hz, and steady-state jitter variance of $3.96 \times 10^4 \text{ Hz}^2$.

results on the transient and steady-state performances are accurate. We can also observe that the convergence of the proposed loop is approximately 18.2 times faster than the conventional first-order loop under the conditions of the identical steady-state jitter variance.

The dotted curves in Fig. 3 show the performance of the second-order loop with an identical damping factor to that of the loop proposed. The pull-in time is slightly reduced compared with the first-order loop, but is still 15.7 times larger than the proposed one.

Now, let us consider another case where $T_A = T_B$ so that the loops have an identical loop update frequency. Similarly to the previous case with $T_A = 2T_B$, the correlation length of the proposed loop should be as small as 8 chips for the identical steady-state jitter variance and, thus, an 8:1 decimation is assumed at the input to the carrier frequency offset estimator. Note that the large decimation ratio results in reduced signal-to-

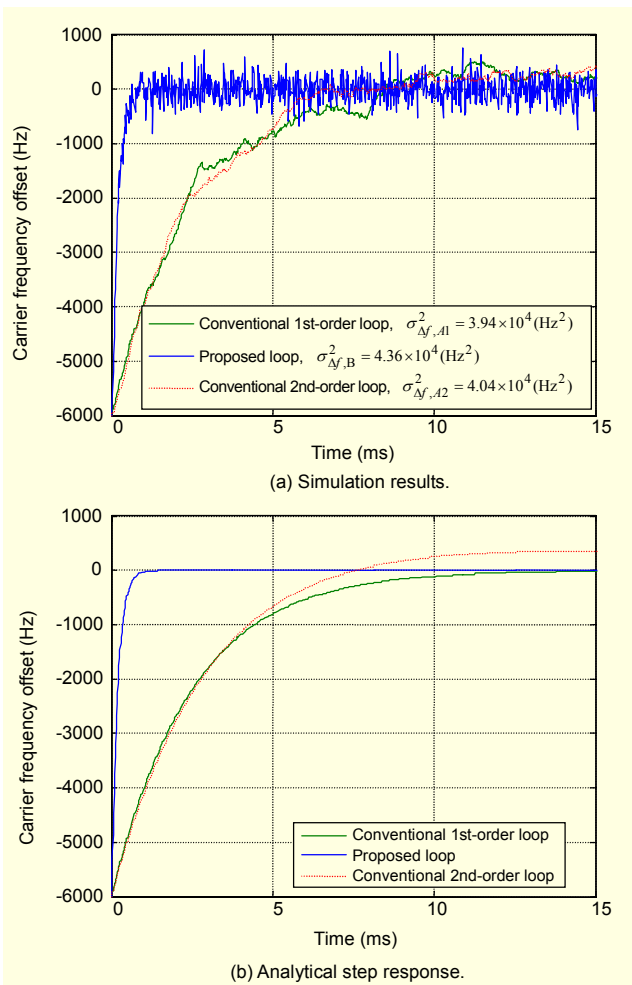


Fig. 4. Loop performances when the loops are designed for identical loop update frequency of 62.5 kHz, equivalent noise bandwidth of 200 Hz, and steady-state jitter variance of $3.96 \times 10^4 \text{ Hz}^2$.

Table 1. Pull-in time performances under identical steady-state jitter variance of $3.96 \times 10^4 \text{ Hz}^2$.

	Pull-in time (ms)		
	Proposed loop	Conventional 1st-order loop	Conventional 2nd-order loop
$T_B = T_A/2$, 2:1 decimated input	0.409	7.45	6.42
$T_B = T_A$, 8:1 decimated input	0.570		6.13

noise ratio at the correlator output although the complexity and power consumption are improved due to the reduced sampling frequency within the frequency offset estimator.

The simulation and analytical results are shown in Figs. 4(a) and 4(b), respectively, from which we can again verify the accuracy of the analytical results in section III. Under the

assumption of the identical steady-state jitter variance, the proposed loop is observed to converge 13.1 and 10.8 times faster than the conventional first- and second-order loops, respectively. All the results are summarized in Table 1.

We can also see that, in all the cases considered in this section, the proposed scheme not only reduces the pull-in time by an order of magnitude but also suppresses overshoots frequently observed in conventional second-order loop operations [3]. In Figs. 3(b) and 4(b), overshoots appear at approximately 8 ms and 7.5 ms for the conventional second-order loop.

On the other hand, if we set the pull-in time of the proposed loop to be identical to that of the conventional loops, the steady-state jitter variance of the proposed loop is observed to be reduced by two orders of magnitude. The numerical results are shown in Table 2.

Finally, the pull-in time simulation results are shown in Table 3 under a two-path channel model for evaluation of the proposed scheme under a multipath channel environment. We arbitrarily assumed that the second path signal is $0.44 + j0.35$ times the first path signal with a delay of $2.5 \mu\text{s}$. From the results, we can see that the proposed scheme still reduces the pull-in time by an order of magnitude under an identical steady-state jitter variance, which is almost doubled due to the multipath channel.

From the results presented in this paper, we can conclude that the simple modification of overlapping the observation

Table 2. Steady-state jitter performances under identical pull-in times.

	Pull-in time (ms)	Steady-state jitter variance (Hz^2)		
		Proposed loop	Conventional 1st-order loop	Conventional 2nd-order loop
$T_B = T_A/2$, 2:1 decimated input	7.45	1.33×10^2	3.94×10^4	-
	6.42	1.78×10^2	-	4.04×10^4
$T_B = T_A$, 8:1 decimated input	7.45	2.78×10^2	3.94×10^4	-
	6.13	6.78×10^2	-	4.05×10^4

Table 3. Pull-in time performances under identical steady-state jitter variance of approximately $7.8 \times 10^4 \text{ Hz}^2$ and a simple two-path channel model.

	Pull-in time (ms)		
	Proposed loop	Conventional 1st-order loop	Conventional 2nd-order loop
$T_B = T_A/2$, 2:1 decimated input	0.34	3.6	3.2
$T_B = T_A$, 8:1 decimated input	0.48		2.8

intervals results in great improvements in both transient and steady-state performances of phase-differential carrier frequency recovery loops, even with reduced complexity and power consumption.

V. Conclusions

In this paper, we have proposed a very simple modification to a conventional phase-differential carrier frequency recovery loop, where the frequency offset estimation is made based on the difference of the average phases over two successive subintervals. The proposed scheme simply overlaps the observation intervals by half and does not require any additional circuitry. Analytical and numerical results presented in this paper show that the simple modification to the conventional first-order loop can reduce either the steady-state jitter variance by more than 20 dB or the pull-in time by an order of magnitude, which are far better than what can be achieved by increasing the order of the conventional loop.

Although we have considered a carrier frequency recovery loop for DS-SS signals as an example, the proposed modification can be applied to any other synchronization loops of similar structure.

References

- [1] H. Meyr, M. Moeneclaey, and S. A. Fechtel, *Digital Communication Receivers: Synchronization, Channel Estimation, and Signal Processing*, Wiley, New York, 1998.
- [2] J. K. Holmes, *Coherent Spread Spectrum Systems*, Wiley, New York, 1982.
- [3] H. Meyr and G. Ascheid, *Synchronization in Digital Communications, Volume I: Phase-, Frequency-Locked Loops, and Amplitude Control*, Wiley, New York, 1990.
- [4] M. K. Simon and D. Divsalar, "Doppler-Corrected Differential Detection of MPSK," *IEEE Trans. Commun.*, vol. 37, no. 2, Feb. 1989, pp. 99-109.
- [5] P. H. Moose, "A Technique for Orthogonal Frequency Division Multiplexing Frequency Offset Correction," *IEEE Trans. Commun.*, vol. 42, no. 10, Oct. 1994, pp. 2908-2914.
- [6] T. M. Schmidle and D. C. Cox, "Low-Overhead, Low-Complexity [Burst] Synchronization for OFDM," *Proc. ICC*, June 1996, pp. 1301-1306.
- [7] J. W. Jeong, S. Sampei, and N. Morinaga, "Large Doppler Frequency Compensation Technique for Terrestrial and LEO Satellite Dual Mode DS/CDMA Terminals," *IEICE Trans. Commun.*, vol. E79-B, no. 11, Nov. 1996, pp. 1696-1703.
- [8] T. M. Schmidle and D. C. Cox, "Robust Frequency and Timing Synchronization for OFDM," *IEEE Trans. Commun.*, vol. 45, no. 12, Dec. 1997, pp. 1613-1621.
- [9] In-Gi Lim and Whan-Woo Kim, "A Numerically Controlled Oscillator with a Fine Phase Tuner and a Rounding Processor,"

ETRI Journal, vol. 26, no. 6, Dec. 2004, pp. 657-660.

- [10] F. M. Gardner, "Frequency Granularity in Digital Phase-Locked Loops," *IEEE Trans. Commun.*, vol. 44, no. 6, Jun. 1996, pp. 749-758.



Hyoungsoo Lim received the BS, MS, and PhD degrees in electrical engineering from Pohang University of Science and Technology (POSTECH), Pohang, Korea in 1992, 1994, and 1999, respectively. He was with Radio & Broadcasting Technology Laboratory, Electronics and Telecommunication Research Institute (ETRI), Daejeon, Korea from 1999 to 2000, and DXO Telecom, Inc., Seoul, Korea from 2000 to 2001. He has been with ETRI since 2002 and is now with Digital Broadcasting Research Division, ETRI. His major research interests include synchronizations in digital communications, digital broadcasting signal transmissions, multi-carrier modulation, CDMA, military communications, satellite communications, and wireless LAN/MAN systems.



Dong Seung Kwon received the BS, MS, and PhD degrees in electrical engineering from Yonsei University, Seoul, Korea in 1985, 1987, and 2004. In 1988, he joined ETRI, where he is currently a principal member of research staff and a project manager. He has been involved with the development of the CDMA-based digital cellular system from 1990 to 1995, and participated in the development project of IMT-2000 from 1996 to 2002. From 2003 he was in charge of the development of a physical layer of wireless broadband internet service, which is based on IEEE802.16e specifications. His current research interests are mainly concentrated on digital mobile modems and radio transmission technology of high speed mobile internet.